Inorg. Chem. **2004**, *43*, 5351–5359

Further Mechanistic Information on the Reaction between Fe^{III}(edta) and Hydrogen Peroxide: Observation of a Second Reaction Step and Importance of pH

Ariane Brausam and Rudi van Eldik*

Institute for Inorganic Chemistry, University of Erlangen—Nürnberg, Egerlandstr. 1, 91058 Erlangen, Germany

Received February 24, 2004

A detailed study of the effect of buffer, temperature, and pressure on the reaction of hydrogen peroxide with $[Fe^{III}(edta)H_2O]^-$ was performed using stopped-flow techniques. The reaction was found to consist of two steps and resulted in the formation of the already characterized high-spin Fe(III) side-on bound peroxo complex. The second step of the reaction was found to be independent of the hydrogen peroxide concentration. Formation of the purple peroxo complex is only observable above pH 7.5. Both reaction steps are affected by specific and general acid-catalysis. Five different buffer systems were used to clarify the role of general acid-catalysis in these reactions. Both reaction steps reveal an element of reversibility, which disappears on decreasing the acid concentration. The positive volumes of activation for both the forward and reverse reactions of the first step suggest a dissociative interchange substitution process for the reversible end-on binding of hydrogen peroxide to $[Fe^{III}(edta)H_2O]^-$. The small negative volume of activation for the second reaction step suggests an associative interchange mechanism for the formation of the side-on bound peroxo complex that is accompanied by dissociation of one of the four carboxylates of edta. A detailed mechanism in agreement with all the reported kinetic data is presented.

Introduction

Over the past two decades, the mechanism of oxygen activation by non-heme iron enzymes received much attention, and evidence was presented that iron peroxo species play a key role in these processes.[1] Peroxo intermediates have been characterized spectroscopically for diiron enzymes such as ribonucleotide reductase and methane monooxygenase.[2] Iron peroxo species have also been postulated for mononuclear iron enzymes such as Fe-based superoxide dismutase,[3,4] and on the basis of pulse radiolysis studies for superoxide reductase.[5,6] Another example for a mononuclear iron peroxo species is the activated form of the antitumor drug bleomycin, which shows DNA-cleavage activity when exposed to oxygen. This activated form has been shown to be a hydroperoxo Fe−OOH species.[7] Significant efforts have been undertaken to develop functional models for non-heme iron enzymes. Until now, no mononuclear Fe(III) peroxo complex could be isolated, although several of these species have been generated in solution and characterized by various spectroscopic techniques.[8]

One long known iron peroxo complex is the purple complex $[Fe^{III}(edta)(\eta^2\text{-}O_2)]^{3-}$, which is formed upon addition of H_2O_2 to $Na[Fe^{III}(edta)]$. This complex, which was first studied in 1956,[9] was shown to catalyze the oxidation of organic substrates,[10] the polymerization of styrene,[11] and the decomposition of H_2O_2.[11,12] Furthermore, it acts as a mimic for superoxide dismutase.[13] The binding mode of hydrogen peroxide in the high spin[10] Fe−edta−peroxo complex has been identified as η^2-side-on by resonance Raman spectroscopy.[14] This binding mode is sometimes referred to as the Griffiths mode.[15] $[Fe^{III}(edta)(\eta^2\text{-}O_2)]^{3-}$ was recently charac-

* To whom correspondence should be addressed. E-mail: vaneldik@chemie.uni-erlangen.de.

(1) Costas, M.; Mehn, M. P.; Jehnsen, M. P.; Que, L. *Chem. Rev.* **2004**, *104*, 939−986.
(2) Solomon, E. I.; Brunold, T. C.; Davis, M. I.; Kemsley, J. N.; Lee, S.-K.; Lehnert, N.; Neese, F.; Skulan, A. J.; Yang, Y.-S.; Zhou, J. *Chem. Rev.* **2000**, *100*, 235−349.
(3) Bull, C.; Fee, J. A. *J. Am. Chem. Soc.* **1985**, *107*, 3295−3304.
(4) Dooley, D. M.; Karas, J. L.; Jones, T. F., Coté, C. E.; Smith, S. B. *Inorg. Chem.* **1986**, *25*, 4761−4766.
(5) Lombard, M.; Houée-Levin, C.; Touati, D.; Fontecave, M.; Nivière, V. *Biochemistry* **2001**, *16*, 5032−5040.
(6) Clay, M. D.; Jenney, F. E.; Hagedoorn, P. L.; George, G. M.; Adams, M. W. W.; Johnson, M. K. *J. Am. Chem. Soc.* **2002**, *124*, 788−805.
(7) Sam, J. W.; Tang, X. J.; Peisach, J. *J. Am. Chem. Soc.* **1994**, *116*, 5250−5256.

10.1021/ic0497580 CCC: $27.50
Published on Web 07/17/2004

terized in more detail by the application of a variety of techniques such as Mössbauer,[16] low-temperature absorption, variable temperature−variable magnetic field circular dichroism (VTVH MCD), and electron paramagnetic resonance (EPR) spectroscopy.[17] In combination with theoretical studies,[17] the side-on geometry of the complex was confirmed and the electronic structure was claimed to best match a six-coordinate model, i.e., a structure in which two of the four carboxylates of edta are dissociated from the metal center. This profound knowledge on the Fe−edta−peroxo complex stimulated our interest in the actual mechanism of hydrogen peroxide activation by $[Fe^{III}(edta)H_2O]^-$. Although kinetic information and corresponding mechanistic considerations are available,[10,13,18] some mechanistic details still remained unclear and called for further clarification.

In this study, a more detailed kinetic investigation of the reaction between $[Fe^{III}(edta)H_2O]^-$ and H_2O_2 was performed. As reported before,[13] the reaction turned out to be catalyzed by general acids such that pH plays a major role in controlling the overall reaction sequence as well as the stability of intermediate and product species. Reported for the first time is a second reaction step following the initial coordination of hydrogen peroxide that is independent of the hydrogen peroxide concentration, and also showed general acid-catalysis. A series of different buffer systems were employed to establish the nature of the general acid-catalysis. The effect of temperature and pressure on the kinetics of the activation of hydrogen peroxide was investigated for both reactions, and the activation parameters ($\Delta H^{\ddagger}$, $\Delta S^{\ddagger}$, and $\Delta V^{\ddagger}$) are reported. The applied techniques provide further insight into the underlying reaction mechanism, and an overall reaction scheme is postulated that is in agreement with all the experimental observations for the formation of the Fe−edta−peroxo complex, $[Fe^{III}(edta)(\eta^2\text{-}O_2)]^{3-}$.

Experimental Section

Solutions of $[Fe^{III}(edta)H_2O]^-$ were prepared from solid $Na[Fe^{III}(edta)]$ (Fluka). In all solutions, an equimolar quantity of $Na_2(H_2edta)$ (Aldrich) was present to prevent precipitation of iron hydroxide at higher pH values. An up to 6-fold excess of $Na_2(H_2edta)$ did not have a meaningful influence on the observed kinetic behavior. $NaClO_4$ (Aldrich) was used to adjust the ionic strength. The employed buffers, viz. 3-(cyclohexylamino)propansulfonic acid (CAPS), [tris(hydroxymethyl)methyl]aminopropansulfonic acid (TAPS), glycine, 2-aminoethansulfonic acid (taurine), and *N*-(1,1-dimethyl-2-hydroxyethyl)-3-amino-2-hydroxy-propansulfonic acid (AMPSO) were purchased from Roth. NaOH (Acros Organics) was used to adjust the pH of the buffer solutions. Solutions of H_2O_2 were prepared by dilution of a 35% stock solution of H_2O_2 (Acros Organics). To verify the reproducible concentration of the H_2O_2 stock solution, kinetic measurements were performed regularly at a fixed H_2O_2 concentration throughout the study. No changes in the values of the rate constants were observed, from which it could be concluded that the concentration of H_2O_2 remained constant throughout the measurements. All chemicals were of the highest quality commercially available and used without further purification. All solutions were prepared with deionized water.

pH measurements were performed on a Metrohm 632 pH meter equipped with a Mettler Toledo InLab 422 glass electrode, which was filled with NaCl instead of KCl to prevent precipitation of $KClO_4$.

UV−vis spectra were recorded on Shimadzu UV-2101PC, Varian Cary 1G UV−vis, and Cary 5G UV−vis−NIR spectrophotometers. Kinetic measurements were performed with a thermostated (± 0.1 °C) SX-18 MV (Applied Photophysics) stopped-flow spectrometer. Absorbance changes were recorded at 361 and 505 nm.

Stopped-flow experiments at pressures up to 170 MPa were performed on a custom built instrument described before.[19,20] Kinetic traces were recorded on an IBM-compatible computer and analyzed with the OLIS KINFIT (Bogart, GA, 1989) set of programs.

All kinetic measurements were performed under pseudo-first-order conditions, i.e., at least a 10-fold excess of hydrogen peroxide was employed. Reported rate constants are the mean values from at least five kinetic runs.

Results and Discussion

Spectroscopic Studies. The UV−vis spectrum of $[Fe(edta)H_2O]^-$ measured in 0.35 M TAPS buffer at pH = 9 exhibits an absorption maximum at 243 nm (ϵ = 7500 M^{-1} cm^{-1}), in agreement with that reported in the literature.[21,13] The high buffer concentration was required in order to control the pH under various experimental conditions. Unless otherwise stated, the concentration of the buffer was 0.35 M throughout the measurements.

Fe(III)−edta is hepta-coordinate in the crystalline state with an approximate pentagonal-bipyramidal structure.[22,23]

(8) (a) Bernal, I.; Jensen, I. M.; Jensen, K. B.; McKenzie, C. J.; Toftlund, H.; Tuchagues, J. P. *J. Chem. Soc., Dalton Trans.* **1995**, 3667−3675. (b) Kim, C.; Chen, K.; Kim, J.; Que, L. *J. Am. Chem. Soc.* **1997**, *119*, 5964−5965. (c) Lubben, M.; Meetsmea, A.; Wilkinson, E. C.; Feringa, B.; Que, L. *Angew. Chem., Int. Ed. Engl.* **1995**, *34*, 2048−2051. (d) Zhang, Y.; Elgren, T. E.; Dong, Y.; Que, L. *J. Am. Chem. Soc.* **1993**, *115*, 811−813. (e) Jensen, K. B.; McKenzie, C. J.; Nielsen, L. B.; Pedersen, J. Z.; Svendsen, H. M. *Chem. Commun.* **1999**, 1313−1314. (f) Simaan, A. J.; Banse, F.; Mialane, P.; Boussac, A.; Un, S.; Kargar-Grisel, T.; Bouchoux, G.; Girerd, J.-J. *Eur. J. Inorg. Chem.* **1999**, 993−996. (g) Simaan, A. J.; Döpner, S.; Banse, F.; Bourcier, S.; Bouchoux, G.; Boussac, A.; Hildebrandt, P.; Girerd, J.-J. *Eur. J. Inorg. Chem.* **2000**, 1627−1633. (h) Hazell, A.; McKenzie, C. J.; Nielsen, L. B.; Schindler, S.; Weitzer, M. *J. Chem. Soc., Dalton Trans.* **2002**, 3010−3017. (i) Balland, V.; Banse, F.; Anxokabehere-Mallart, E.; Ghiladi, M.; Mattioli, T. A.; Philouze C.; Blondin, G.; Girerd, J.-J. *Inorg. Chem.* **2003**, *42*, 2470−2477.

(9) Cheng, K. L.; Lott, P. F. *Anal. Chem.* **1956**, *28*, 462−465.

(10) (a) Walling, C.; Kurz, M.; Schugar, H. J. *Inorg. Chem.* **1970**, *9*, 931−937. (b) Walling, C. *Acc. Chem. Res.* **1975**, *8*, 125−131. (c) Walling, C.; Kato, S. J. *J. Am. Chem. Soc.* **1971**, *93*, 4275−4281.

(11) Bond, J.; Brown, C. W.; Rushton, G. S. *Polymer Lett.* **1964**, *2*, 1015−1017.

(12) Kachanova, Z. P.; Purmal, A. P. *Russ. J. Phys. Chem.* **1964**, *38*, 2506−2508.

(13) Bull, C.; McClune, G. J.; Fee, J. A. *J. Am. Chem. Soc.* **1983**, *105*, 5290−5300.

(14) (a) Hester, R. E.; Nou, E. M. *J. Raman Spectrosc.* **1981**, *11*, 35−38. (b) Ahmad, S.; McCallum, J. D.; Shiemke, A. K.; Appelman, E. H.; Loehr, T. M.; Sanders-Loehr, J. *Inorg. Chem.* **1988**, *27*, 2230−2233.

(15) Griffith, J. S. *Proc. R. Soc. London, Ser. A* **1956**, *235*, 23.

(16) Horner, O.; Jeandey, C.; Oddou, J. L.; Bonville, P.; Latour, J.-M. *Eur. J. Inorg. Chem.* **2002**, 1186−1189.

(17) Neese, F.; Solomon, E. I. *J. Am. Chem. Soc.* **1998**, *120*, 12829−12848.

(18) Francis, K. C.; Cummins, D.; Oakes, J. *J. Chem. Soc., Dalton Trans.* **1985**, 493−501.

(19) van Eldik, R.; Palmer, D. A.; Schmidt, R.; Kelm, H. *Inorg. Chim. Acta* **1981**, *50*, 131−135.

(20) van Eldik, R.; Gaede, W.; Wieland, S.; Kraft, J.; Spitzer, M.; Palmer, D. A.; *Rev. Sci. Instrum.* **1993**, *64*, 1355−1257.

(21) Dellert-Ritter, M.; van Eldik, R. *J. Chem. Soc., Dalton Trans.* **1992**, 1037−1344.

As a result of the coordinated water molecule in the seven-coordinate $[Fe^{III}(edta)H_2O]^-$,[24−26] this complex exhibits a characteristic acid−base equilibrium in aqueous solution. A pH titration between pH = 2.0 and 11.0 provided evidence for a single deprotonation step, which can be assigned to reaction 1. The pK_1 value was determined to be 7.4 at 25 °C, which is in good agreement with results reported in the literature.[21,27]

$$[Fe(edta)(H_2O)]^- \overset{K_1}{\rightleftharpoons} [Fe(edta)(OH)]^{2-} + H^+ \qquad (1)$$

On the basis of earlier potentiometric studies of the hydrolysis equilibria,[27,28] the formation of a dimer via reaction 2 was proposed. Each iron center of the oxo bridged dimer both in the solid state and in aqueous solution is six-coordinate with a quinquedentate edta ligand.[29] The Fe−O−Fe bridge exhibits an approximate linear geometry.[28] Formation of a shoulder at 470 nm in the UV−vis spectrum above pH 7.0 indicates dimerization according to eq 2. The dimerization is only evident at higher complex concentrations. When working in a millimolar concentration range, no shoulder at 470 nm can be observed and only the monomeric hydroxo species is formed above pH 7.0.

$$2[Fe(edta)(H_2O)]^{2-} \overset{K_2}{\rightleftharpoons} [(edta)-Fe-O-Fe(edta)]^{4-} + H_2O \qquad (2)$$

Upon addition of H_2O_2 to a buffered solution of $[Fe^{III}(edta)]^-$ at pH above 8.0, a band with λ_{max} = 520 nm is formed, which can be assigned to the formation of the purple Fe−edta−peroxo complex. The purple color is ascribed to an LMCT band of the side-on bound peroxo complex.[10,17] Below a pH of ca. 8, no overall reaction is observed (see further discussion).

Figure 1 shows the spectral changes observed during the reaction of hydrogen peroxide with $[Fe^{III}(edta)]^-$ at high pH, which are in good agreement with earlier reports.[10,17] The intensity of the band at 520 nm at first increases rapidly and then in a second stage increases much more slowly. A comparison of kinetic traces recorded at two different wavelengths shows this even more clearly (see inset in Figure 1). The absorbance at 361 nm exhibits a rapid increase followed by a subsequent slow decrease. The latter step is characterized by an isosbestic point at 420 nm.

The observed rate constant for the second slow reaction turned out to be independent of the hydrogen peroxide concentration. Presumably, it can be assigned to an intramolecular rearrangement reaction of an intermediate complex produced in the first reaction step. Due to the larger spectral changes, the second reaction step was followed at 361 nm in contrast to 505 nm being used for the observation of the first reaction step. The reaction sequence in eq 3 is formulated as a working hypothesis:

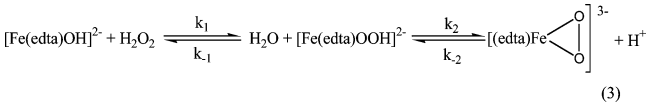

(3)

In this overall reaction, the first reaction step involves the reversible end-on coordination of H_2O_2, followed by the subsequent formation of side-on coordinated peroxide.

Kinetic Studies: Investigation of the First Reaction Step. The kinetics of this reaction was studied by stopped-flow spectrometry. As known from earlier studies,[13] the reaction of hydrogen peroxide with $[Fe^{III}(edta)]^-$ is sensitive to general acid-catalysis. The effect of five different buffers on k_{1obs} was investigated. Kinetic data were obtained under pseudo-first-order conditions, $[H_2O_2] \gg [Fe(edta)^-]$. None of the employed buffers showed any interaction with the starting material.[13] Unless otherwise stated, the concentration of the buffer was 0.35 M throughout the measurements.

Kinetic traces recorded in the presence of an excess of H_2O_2 showed a two-step behavior that could be fitted by two exponential functions. The time scale of the two steps was such that the reaction could be separated into two steps by selecting different time scales and fitting each step to a single-exponential function. Typical kinetic traces and the corresponding fits for the two reaction steps are shown in Figure S1 and S2 (see Supporting Information).

Plots of k_{1obs} versus the H_2O_2 concentration at different buffer concentrations (a typical example is given in Figure 2 for TAPS) were found to be linear with a significant intercept. The rate law for this reaction based on the first reaction step outlined in eq 3 is given in eq 4. The overall spectral changes increased significantly with increasing hydrogen peroxide concentration, from which it followed that

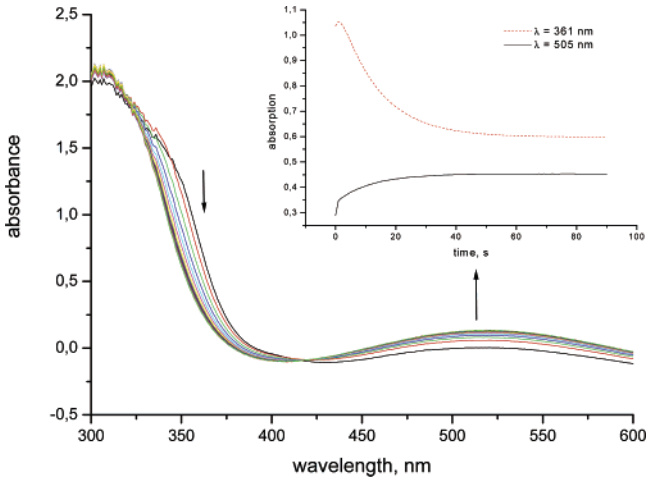

Figure 1. Spectral changes for the reaction of $[Fe^{III}(edta)]^-$ with H_2O_2 at pH 10.5 (CAPS). Experimental conditions: $[Fe(edta)^-]$ = 0.001 M, $[H_2O_2]$ = 0.01 M, I = 0.5 M, T = 2.5 °C. Inset: Kinetic traces for the reaction of $[Fe^{III}(edta)]^-$ with H_2O_2.

(22) Hoard, J. L.; Lind, M.; Silverton, J. V. *J. Am. Chem. Soc.* **1961**, *83*, 2770−2771.
(23) Lind, M. D.; Hoard, J. L.; Hamor, M. J.; Hamor, T. A. *Inorg. Chem.* **1964**, *3*, 34−43.
(24) Whidby, J. F.; Leyden, D. E. *Anal. Chim. Acta* **1970**, *51*, 25−30.
(25) Oakes, J.; Smith, E. G. *J. Chem. Soc., Faraday Trans. 1* **1983**, 543−552.
(26) Francis, K. C.; Cummins, D.; Oakes, J. *J. Chem. Soc., Dalton Trans.* **1985**, 493−501.
(27) Gustafson, R. L.; Martell, A. E. *J. Phys. Chem.* **1963**, *67*, 576−582.
(28) Schugar, H. J.; Hubbard, A. T.; Anson, F. C.; Gray, H. B. *J. Am. Chem. Soc.* **1969**, *91*, 71−77.
(29) Kanamori, K.; Dohniwa, H.; Ukita, N.; Kanesaka, I.; Kawai, K. *Bull. Chem. Soc. Jpn.* **1990**, *63*, 1447−1454.

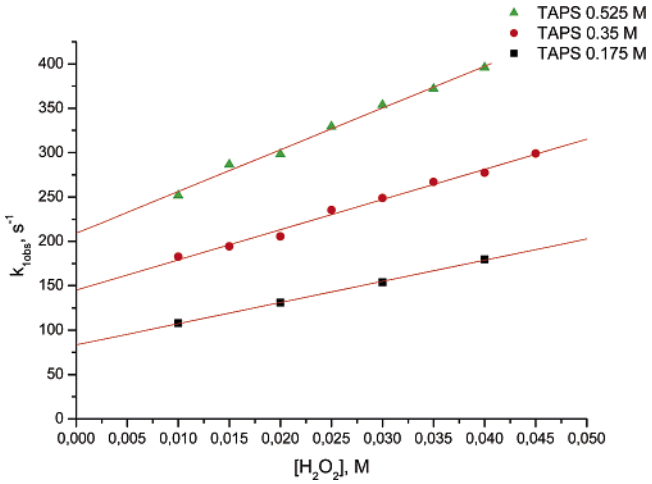

Figure 2. Plots of k_{1obs} versus [H_2O_2] at pH = 9.0 (TAPS) as a function of the buffer concentration. Experimental conditions: [Fe(edta)$^-$] = 0.001 M, I = 0.5 M, T = 25 °C.

coordination of hydrogen peroxide is a reversible process. Under conditions where the dead time of the stopped-flow instrument (ca. 4 ms) does not interfere with the spectral changes observed during the kinetic traces, i.e., for the data obtained at 0.175 M TAPS in Figure 2, an apparent thermodynamic equilibrium constant of 38 ± 3 M^{-1} was calculated from the spectral changes observed for the first step in reaction 3, which is in close agreement with the kinetic value for k_1/k_{-1} of 29 ± 3 M^{-1} under these conditions (see Figure 2).

$$k_{1obs} = k_{-1} + k_1[H_2O_2] \quad (4)$$

Both the intercept (k_{-1}) and slope (k_1) are affected by increasing buffer concentration. More information on the buffer dependence of k_1 and k_{-1} was obtained from similar plots as shown in Figure 2 for the different buffers employed. In fact, it turned out that both k_1 and k_{-1} depend on the concentration of the acidic form of the buffer, which is abbreviated as BH^+ in the remainder of the text.

Plots of k_1 versus [BH^+] at a fixed pH are linear (see Figure 3) and exhibit intercepts that in turn show an acid-dependence as shown in Figure S3 (Supporting Information). The latter plot suggests that there is a meaningful intercept that can be ascribed to the contribution of a spontaneous reaction path. The buffer concentration and pH dependence of k_1 can therefore be described by eq 5, where k_{H_2O} represents the non-acid-catalyzed, spontaneous reaction path, k_{1H} the acid-catalyzed reaction path, and k_{1BH} the general acid-catalyzed reaction path for the formation of [Fe(edta)OOH]$^{2-}$.

$$k_1 = k_{H_2O} + k_{1H}[H^+] + k_{1BH}[BH^+] \quad (5)$$

From Figure S3 it follows that k_{H_2O} = 170 ± 190 M^{-1} s^{-1} and k_{1H} = 6 ± 3 M^{-2} s^{-1}. Compared to general acid-catalysis with $k_{1BH} = 1.3 \times 10^3$ to 2.8×10^4 M^{-2} s^{-1}, proton catalysis plays a minor role in this reaction step. The value of k_{H_2O} is in relatively good agreement with 350 M^{-1} s^{-1} for the non-acid-catalyzed reaction reported in the literature.[13] The slopes of the lines in Figure 3, k_{1BH} (M^{-2} s^{-1}), correlate with the

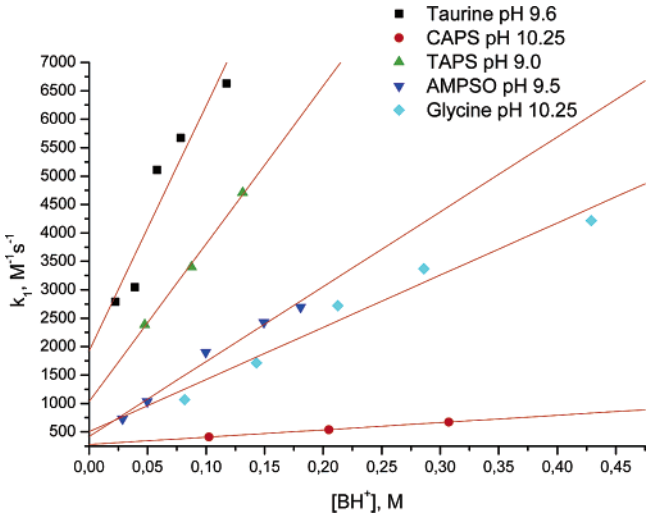

Figure 3. Plots of k_1 versus [BH^+] for different selected buffers. Experimental conditions: [Fe(edta)$^-$] = 0.001 M, [H_2O_2] = 0.01−0.04 M, I = 0.5 M, T = 25 °C.

Table 1. Summary of Rate Constants for the General Acid-Catalyzed Reaction Steps[a]

buffer	pK_a	k_{1BH}, M^{-2} s^{-1}	k_{-1BH}, M^{-1} s^{-1}	k_{-2BH}, M^{-1} s^{-1}
TAPS	8.4	(2.8 ± 0.1) × 10^4	(1.0 ± 0.1) × 10^3	
taurine	9.06	(4.3 ± 0.8) × 10^4	(1.9 ± 0.6) × 10^3	40 ± 2
AMPSO	9.1	(1.3 ± 0.1) × 10^4	(0.4 ± 0.1) × 10^3	
glycine	9.9	(1.2 ± 0.2) × 10^4	(0.3 ± 0.3) × 10^3	5.7 ± 0.6
CAPS	10.4	(1.3 ± 0.3) × 10^3	(0.3 ± 0.1) × 10^3	

[a]Experimental conditions: [Fe(edta)$^-$] = 0.001 M, [H_2O_2] = 0.01−0.04 M, I = 0.5 M, T = 25 °C.

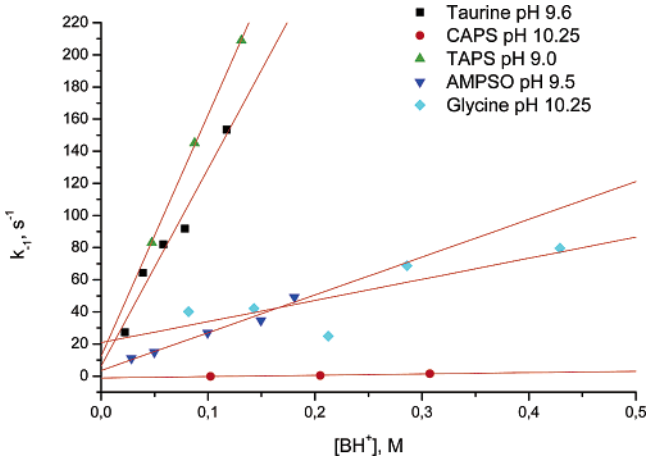

Figure 4. Plots of k_{-1} versus [BH^+] for different selected buffers. Experimental conditions: [Fe(edta)$^-$] = 0.001 M, [H_2O_2] = 0.01−0.04 M, I = 0.5 M, T = 25 °C.

pK_a values of the different buffers (see Figure S4, slope = −0.64, Supporting Information), which in turn determines the effectiveness of the general acid-catalysis contribution. The lower the pK_a value, i.e., the stronger the acid, the higher the corresponding value for k_{1BH} is (see Table 1).

Plots of k_{-1} versus [BH^+] show a linear behavior with almost negligible intercepts (Figure 4), which can be described by eq 6, where the slope k_{-1BH} represents the general acid-catalyzed back reaction. A careful analysis of the intercept of these plots as a function of pH and [H^+] revealed no specific trend as in the case of the values for k_1.

$$k_{-1} = k_{-1BH}[BH^+] \quad (6)$$

Again, there is a good correlation between the pK_a value of the buffers and k_{-1BH}, viz. the smaller the pK_a value, the faster the general acid-catalyzed back reaction (Figure S5, slope −1.1, Supporting Information). In the case of CAPS and glycine as buffers, the back reaction becomes almost insignificant. Presumably, CAPS with a pK_a of 10.4 and glycine with a pK_a of 9.9 are not able to catalyze the back reaction due to their very low acid strength. However, it is important to note that the back reaction (k_{-1}) is more sensitive to general acid-catalysis than the forward reaction (k_1) as seen from a comparison of the slopes in Figures S4 and S5, viz. −0.64 and −1.1, respectively. This was also seen from absorbance changes recorded during the reaction as a function of pH, which clearly decreased on decreasing the pH, thus shifting the equilibrium back to the reactants on decreasing the pH. The formation of the hydroperoxo intermediate cannot be observed anymore at pH ∼ 7.5. It follows that the stability of $[Fe^{III}(edta)OOH]^{2-}$ produced in the first reaction step is controlled by the pH of the solution (see further discussion).

From a combination of all the kinetic data reported above, the observed rate constant for the first reaction step can be expressed as given in eq 7:

$$k_{1obs} = k_{-1HB}[BH^+] + (k_{H_2O} + k_{1H}[H^+] + k_{1BH}[BH^+])[H_2O_2] \quad (7)$$

In agreement with an earlier study,[13] it was found that both forward and back reactions are affected by general acid-catalysis. As reported before, the forward reaction can also proceed via a spontaneous, non-general acid-catalyzed pathway, which involves proton transfer from hydrogen peroxide onto the $[Fe(edta)OH]^{2-}$ species. In addition, evidence for a third pathway for the forward reaction involving catalysis by H^+ was found in this study.

The reaction was also studied as a function of temperature and pressure. Since plots of k_{1obs} versus $[H_2O_2]$ exhibit no intercept at pH > 10.0, the temperature and pressure dependence was investigated at two different pH values, viz. at pH = 9.0 where a back reaction is evident and at pH 10.5 where the back reaction is insignificant. Typical results are shown in Figures 5 and S6 (Supporting Information). The temperature dependence of k_{1obs} as a function of $[H_2O_2]$ at selected pH values was used to construct Eyring plots for k_1 and k_{-1}, from which the activation parameters $\Delta H^{\ddagger}$ and $\Delta S^{\ddagger}$ were determined (see for example Figure S6). The determination of $\Delta S^{\ddagger}$ involves a linear extrapolation to $1/T = 0$, such that the values of $\Delta S^{\ddagger}$ can be subjected to large errors. Consequently, this parameter does not always provide reliable mechanistic information. A more reliable parameter for mechanistic discrimination is the volume of activation, $\Delta V^{\ddagger} = -RT(\mathrm{d} \ln k/\mathrm{d}P)_T$), where $\Delta V^{\ddagger}$ is determined from the slope of a plot of ln k versus pressure and represents the volume of activation for the reaction with rate constant k. The effect of pressure on the reaction of H_2O_2 with $[Fe(edta)H_2O]^-$ was studied as a function of $[H_2O_2]$ in 0.35 M CAPS buffer solution at 2.3 °C over the pressure range 10−130 MPa (see Figure 5). From these data, the volumes of activation for k_1 (slope) and k_{-1} (intercept) were determined. All activation parameters for the forward and back reactions at the selected pH values are summarized in Table 2.

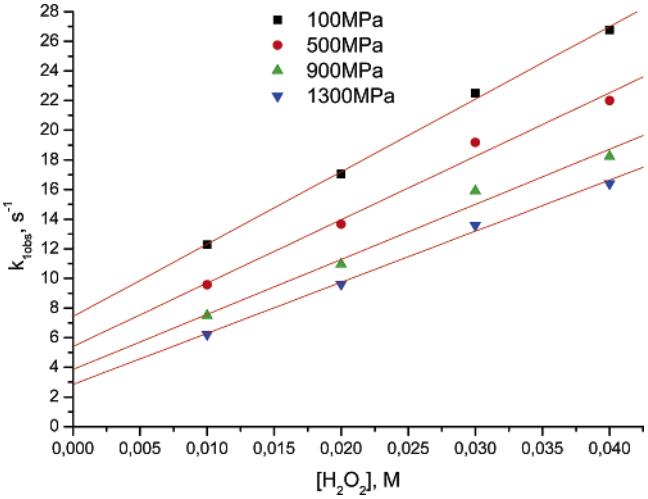

Figure 5. k_{1obs} vs $[H_2O_2]$ as a function of pressure at pH 9.0 (TAPS). Experimental conditions: $[Fe(edta)^-] = 0.001$ M, $[H_2O_2] = 0.01-0.04$ M, $I = 0.5$ M, $T = 2.3$ °C.

Table 2. Summary of Activation Parameters for the Two-Step Reaction[a]

parameter	pH 9.0 k_1	pH 9.0 k_{-1}	pH 10.5 k_1	pH 10.5 k_2	pH 8.5 k_{-2}
$\Delta H^{\ddagger}$, kJ mol^{-1}	+37 ± 4	+101 ± 2	+45 ± 2	+79 ± 2	+86 ± 2
$\Delta S^{\ddagger}$, J K^{-1} mol^{-1}	−53 ± 14	+135 ± 6	−42 ± 5	−10 ± 5	+56 ± 6
$\Delta V^{\ddagger}$, cm^3 mol^{-1}	+6.8 ± 0.8	+18.4 ± 0.6	+6.9 ± 0.3	−2.3 ± 0.1	+5.1 ± 0.2

[a] Experimental conditions: $[Fe(edta)^-] = 0.001$ M, $[H_2O_2] = 0.01-0.04$ M, $I = 0.5$ M.

Table 3. Typical Values for k_{2obs} as a Function of pH and $[H_2O_2]$[a]

pH	H_2O_2, M	k_{2obs}, s^{-1}
9.0 (TAPS)	0.010	1.97 ± 0.02
9.0 (TAPS)	0.040	1.78 ± 0.02
10.0 (CAPS)	0.010	0.690 ± 0.004
10.0 (CAPS)	0.040	0.690 ± 0.005

[a] Experimental conditions: $[Fe(edta)^-] = 0.001$ M, $[H_2O_2] = 0.01-0.04$ M, $I = 0.5$ M, $T = 25$ °C.

Investigation of the Second Reaction Step. The kinetics of this reaction was studied by stopped-flow spectroscopy for five different buffers. The buffer concentration was 0.35 M unless otherwise stated. It follows from Table 3 that the observed rate constant of this reaction (k_{2obs}) is independent of the hydrogen peroxide concentration. Presumably, this reaction involves an intramolecular rearrangement to the well characterized $[Fe^{III}(edta)(\eta^2\text{-}O_2)]^{3-}$ complex.[14,16,17]

Again, the absorbance changes at pH = 9.0 in TAPS buffer are significantly larger than those at pH = 8.5, indicating that the reaction is suppressed by an increase in acidity. The same is true for glycine and CAPS as buffer. In the case of CAPS, this effect is very small, suggesting that the back reaction is almost insignificant in this buffer. These absorbance changes suggest that k_{2obs} consists of two opposing reactions, for which the back reaction seems to be more affected by general acid-catalysis. It is concluded from mech-

Table 4. Typical Values for k_{2obs} as a Function of Buffer Concentration[a]

pH	buffer	buffer, [M]	k_{2obs}, [s^{-1}]
9.0	TAPS	0.175	1.97 ± 0.03
		0.35	1.97 ± 0.02
8.9	taurine	0.175	7.2 ± 0.1
		0.35	9.7 ± 0.1
9.5	AMPSO	0.35	0.76 ± 0.01
		0.525	0.75 ± 0.09
10.25	glycine	0.175	0.33 ± 0.01
		0.35	0.439 ± 0.002
10.25	CAPS	0.175	0.121 ± 0.001
		0.35	0.105 ± 0.001

[a] Experimental conditions: [Fe(edta)$^-$] = 0.001 M, [H_2O_2] = 0.01−0.04 M, I = 0.5 M, T = 25 °C.

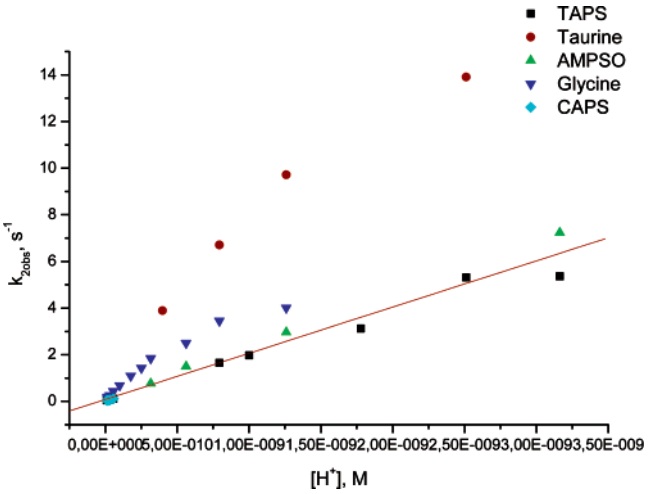

Figure 6. Plot of k_{2obs} vs [H$^+$]. Experimental conditions: [Fe(edta)$^-$] = 0.001 M, [H_2O_2] = 0.01 M, I = 0.5 M, T = 25 °C.

anistic considerations discussed in more detail below that only the back reaction is affected by general acid-catalysis.

For the second reaction step, a different dependence on the employed buffer concentration was observed as for the first reaction step. It turned out that the rearrangement reaction is only affected by general acid-catalysis when taurine or glycine buffers were employed. For example, in 0.175 M glycine buffer, k_{2obs} is 0.330 ± 0.008 s^{-1}, increases to 0.440 ± 0.002 s^{-1} in 0.35 M glycine, and to 0.520 ± 0.007 s^{-1} in 0.525 M glycine. Typical values for k_{2obs} are summarized in Table 4. Thus, general acid-catalysis also applies to the second reaction step, but only under certain conditions.

As mentioned above, it follows from mechanistic considerations that only the back reaction, i.e., protonation of the Fe(edta)−peroxo complex, is affected by general acid-catalysis. Obviously, this peroxo complex is a sterically constrained species, and only sterically unhindered buffers are capable of protonating it. Of the buffers used in this study, taurine and glycine both have a primary amine function and thus are appropriate for general acid-catalysis. On the other hand, TAPS, AMPSO, and CAPS have secondary amine functions and are sterically too constrained to function as a proton donor.

In Figure 6 it can again be seen that k_{2obs} versus [H$^+$] concentration gives a straight line for the three buffers with a secondary amine function. In the case of the two amino

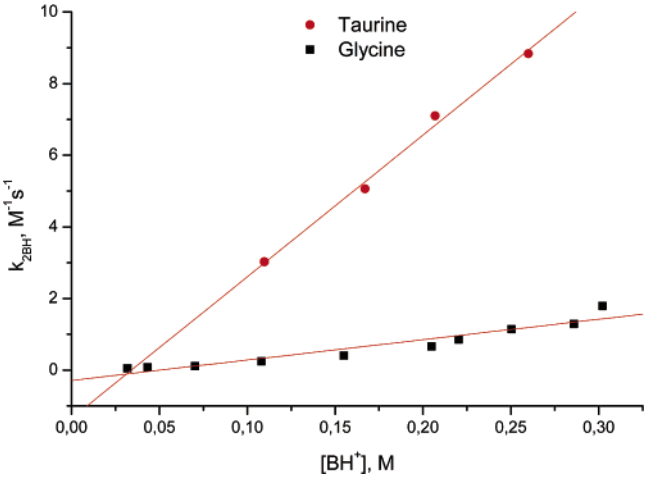

Figure 7. Plots of k_{2HB} vs [BH$^+$]. Experimental conditions: [Fe(edta)$^-$] = 0.001 M, [H_2O_2] = 0.01−0.04 M, I = 0.5 M, T = 25 °C.

acids, a plot of k_{2obs} versus [H$^+$] gives a nonlinear behavior, indicating that there must be another factor that influences k_{2obs}. Plotting the difference between the proton-assisted catalysis and the curved [H$^+$]-dependence for taurine and glycine, against the general acid concentration, as indicated in Figure 7, produces two straight lines. The slopes of the lines represent the general acid-catalyzed back reaction, viz. k_{-2BH}. These lines show no intercept, which means that there is no spontaneous back reaction. As seen for the first reaction step, there is again a correlation between the value of k_{-2BH} and the pK_a of the buffer used, viz. the smaller the pK_a value, the faster the reaction.

At pH > 10.0, the back reaction is almost irrelevant in CAPS and glycine buffers. This is confirmed by the absence of differing absorption changes at pH 10.0 and 10.5. The [BH$^+$] and [H$^+$] concentrations are too small to have any catalytic impact. No acid-catalyzed back reaction is observed, and only the forward reaction is relevant.

The influence of temperature and pressure on this reaction was studied, and typical results are shown in Figures S7 and S8, respectively (Supporting Information).

Kinetic data for the pressure dependence were measured at pH 10.5 (CAPS) and 8.5 (TAPS), where only the forward and back reactions contribute significantly, respectively. The temperature dependence of k_{2obs} was used to construct a linear Eyring plot from which $\Delta H^{\ddagger}$ and $\Delta S^{\ddagger}$ were obtained (Figure S7). The volume of activation was derived from the slope of the linear plot of ln k_{2obs} versus pressure at 25 °C in the pressure range 10−170 MPa (Figure S8). All activation parameters for the rearrangement reaction are summarized in Table 2.

The reported volumes of activation can be used to construct a volume profile (Figure 8) for the overall reaction in eq 3 and detailed mechanism presented in Scheme 1. The positive activation volume, $\Delta V^{\ddagger}$ = +6.8 ± 0.4 cm^3 mol^{-1}, suggests an I_d mechanism for the ligand substitution reaction on [Fe(edta)OH]$^-$ with hydrogen peroxide. The back reaction seems to have a stronger dissociative character on the basis of the significantly positive values for both $\Delta V^{\ddagger}$ (+18.4 cm^3 mol^{-1}) and $\Delta S^{\ddagger}$ (+135 ± 6 J K^{-1} mol^{-1}). For the second

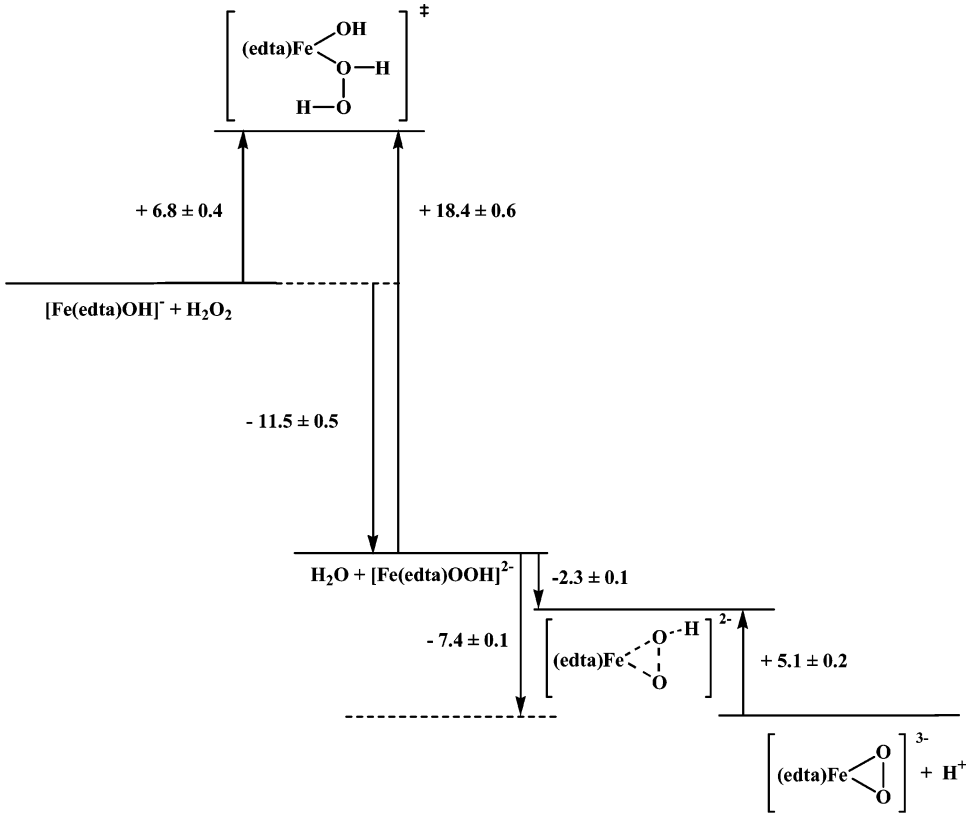

Figure 8. Volume profile for the overall reaction in eq 3.

reaction step, a slightly negative $\Delta V^{\ddagger}$ (-2.3 ± 0.1 cm^3 mol^{-1}) for the intramolecular rearrangement (from end-on to side-on bound peroxide) was found, which is in agreement with an associative interchange type of peroxide chelation reaction. The reverse peroxide dechelation reaction of the $[Fe^{III}(edta)(\eta^2\text{-}O_2)]^{3-}$ peroxo complex is suggested to follow a dissociative interchange type of reaction since $\Delta V^{\ddagger}$ has a small positive value of $+5.1 \pm 0.2$ cm^3 mol^{-1}. During the peroxide chelation and dechelation reactions, we propose that one of the four carboxylates on edta dissociates from and associates with the metal center, respectively, such that a seven-coordinate geometry is maintained throughout the process (see further discussion).

In recent studies,[8h,i] $\Delta S^{\ddagger}$ and $\Delta H^{\ddagger}$ values for the formation of a $[Fe^{III}L_5(OOH)]^{2+}$ complex in nonaqueous solution were reported. The negative values for $\Delta S^{\ddagger}$ probably point to a mechanism with an associative character for the formation of the hydroperoxo species, although it is not advisable to propose a mechanism only on the basis of $\Delta S^{\ddagger}$ data.

Suggested Reaction Mechanism. Scheme 1 shows the suggested mechanism for the overall reaction on the basis of the obtained data.

The formation of the $[Fe^{III}(edta)(\eta^2\text{-}O_2)]^{3-}$ peroxo complex is only observed at pH values significantly larger than the pK_a value of $[Fe(edta)H_2O]^-$. This suggests that the main reacting species in solution is $[Fe(edta)OH]^{2-}$. This is in agreement with the findings in several other studies in the literature.[13,18] The $[Fe(edta)OH]^{2-}$ complex can either be protonated by H^+ ions or by the acidic form of the buffer, BH^+. Proton catalysis involves the formation of $[Fe(edta)H_2O]^-$, which is more labile than $[Fe(edta)OH]^{2-}$ and can react rapidly with H_2O_2, followed by the deprotonation of coordinated H_2O_2 to produce the hydroperoxy product. As compared to the BH^+ concentration, the concentration of protons in solution is small. Thus, although specific acid-catalysis is evident (Figure S3), general acid-catalysis by BH^+ plays a more important role. Protonation of $[Fe(edta)OH]^{2-}$ to form $[Fe(edta)H_2O]^-$ involves charge neutralization and may result in a positive contribution to $\Delta V^{\ddagger}$. It is known from the literature[30] that the water exchange reaction on $[Fe(edta)H_2O]^-$ follows a dissociative interchange (I_d) mechanism characterized by a small positive $\Delta V^{\ddagger}$ value of $+3.2 \pm 0.4$ cm^3 mol^{-1}. This is in close agreement with the observed volume of activation for k_1, viz. $\Delta V^{\ddagger} = +6.9 \pm 0.5$ cm^3 mol^{-1} at pH 10.5 when a positive contribution from charge neutralization due to general acid-catalysis is taken into account. Thus, complex-formation with H_2O_2 also follows an I_d mechanism as found for water exchange on the aqua complex.

It is reasonable to expect that the pK_a value of coordinated hydrogen peroxide in the $[Fe^{III}(edta)(H_2O_2)]^-$ complex will be a few units lower than that for free H_2O_2, viz. 11.6, due to the electron withdrawing effect of the positively charged metal center. Therefore, the $[Fe^{III}(edta)(H_2O_2)]^-$ complex can be stabilized as $[Fe^{III}(edta)OOH]^{2-}$ as a result of deprotonation at high enough pH. Such hydroperoxo intermediates were also suggested for other non-heme iron complexes.[31,32]

(30) Schneppensieper, T.; Seibig, S.; Zahl, A.; Tregloan, P.; van Eldik, R. *Inorg. Chem.* **2001**, *40*, 3670−3676.

Scheme 1

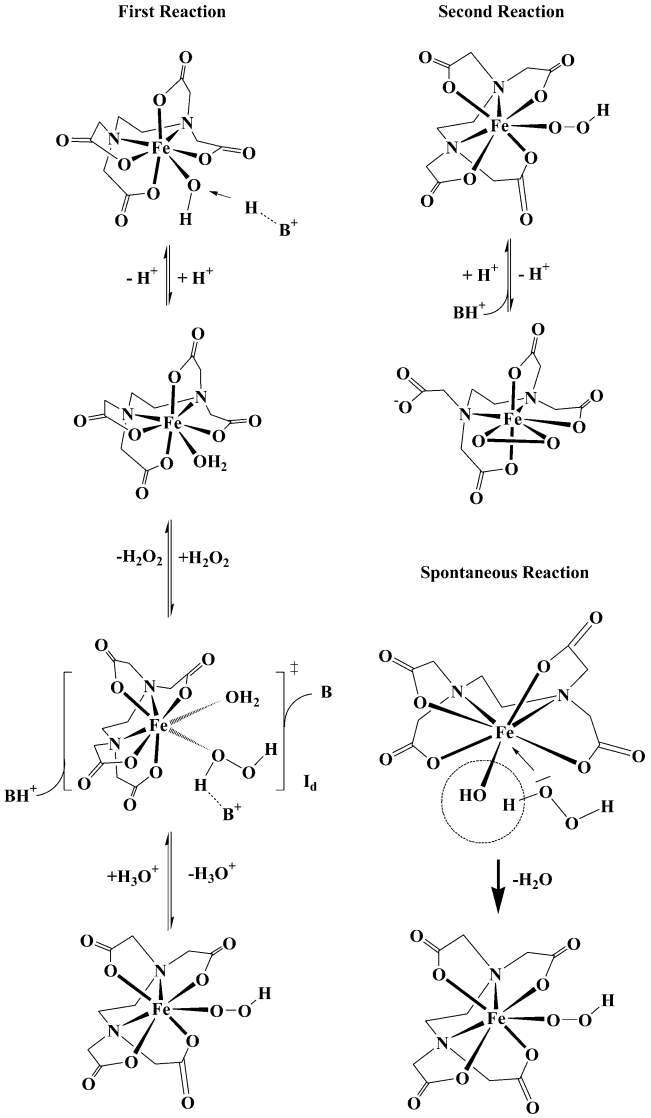

As mentioned before, the back reaction also shows general acid-catalysis. The acidic form of the buffer protonates the $[Fe^{III}(edta)OOH]^{2-}$ complex, and hydrogen peroxide dissociates. This reaction also proceeds via a dissociative mechanism as supported by $\Delta V^{\ddagger} = +18.4 \pm 0.6$ cm^3 mol^{-1} and $\Delta S^{\ddagger} = +135 \pm 6$ J K^{-1} mol^{-1}. If the pK_a value of the buffer is too high as in the case of CAPS, or if the BH^+ concentration is too low, then protonation of the hydroperoxo complex cannot occur and no back reaction is observed.

After the formation of the end-on bound hydroperoxo complex, the $[H_2O_2]$-independent rearrangement to the well characterized side-on bound $[Fe^{III}(edta)(\eta^2\text{-}O_2)]^{3-}$ complex occurs as a slow subsequent reaction step. The reaction fits an associative interchange (I_a) process that is accompanied by the dissociation of one acetate arm of edta. As expected, such a rearrangement is characterized by small negative values for $\Delta V^{\ddagger}$ and $\Delta S^{\ddagger}$, viz. -2.3 ± 0.1 cm^3 mol^{-1} and -10 ± 5 J K^{-1} mol^{-1}, respectively. The negative values for $\Delta V^{\ddagger}$ and $\Delta S^{\ddagger}$ rule out another possible mechanism, viz. formation of a seven-coordinate end-on peroxo complex that is followed by dechelation of one of the carboxylate arms prior to chelation of the end-on bound peroxide to yield a seven-coordinate side-on bound peroxo complex. Such a pathway would fit a dissociative interchange (I_d) mechanism with significantly positive values for $\Delta V^{\ddagger}$ and $\Delta S^{\ddagger}$. Again, general acid-catalysis is evident, as shown in Scheme 1. It is only the back reaction, viz. the protonation of the side-on peroxo complex that is catalyzed by general acids. This is confirmed by the smaller spectral changes observed for this reaction at higher general acid concentrations. Once again, the back reaction is only significant when the pK_a value is not too high (CAPS) or when the BH^+ concentration is not too low. The back reaction fits a dissociative interchange (I_d) process with the dechelated acetate arm of edta, which is accompanied by positive values for the activation parameters, viz. $\Delta V^{\ddagger} = +5.1 \pm 0.2$ cm^3 mol^{-1} and $\Delta S^{\ddagger} = +56 \pm 6$ J K^{-1} mol^{-1}. As discussed above, general acid-catalysis is only evident in such cases where the buffers used are not sterically hindered. Of the five buffers applied in this study, only taurine and glycine proved to be effective catalysts.

It is difficult on the basis of the available data to draw any conclusions whether edta acts as a penta- or hexadentate ligand in the reactions with hydrogen peroxide. It is known[33] that $[Fe(edta)OH]^-$ in solution exists as an equilibrium between a hexadentate seven-coordinate and a pentadentate six-coordinate form with a noncoordinated carboxylate arm. It is difficult to determine whether the seven- or six-coordinate form is the reactive species. In terms of an I_d type of substitution mechanism for the coordination of hydrogen peroxide, it would be reasonable to expect that the seven-coordinate species is the reactive one. On the other hand, if the six-coordinate species is the reactive form and ring closure of the carboxylate arm occurs during the reaction, this could be a possible explanation for the large negative $\Delta S^{\ddagger}$ value. Such a ring-closure process should result in a significantly negative activation entropy but could have a smaller effect in terms of the activation volume.

The hexadentate seven-coordinate end-on bound hydroperoxo complex could potentially rearrange to $[Fe^{III}(edta)(\eta^2\text{-}O_2)]^{3-}$ in favor of a pentadentate seven-coordinate side-on geometry in which one carboxylate of edta dissociates from the metal center in order to avoid the formation of an eight-coordinate Fe(III) complex. As mentioned above, theoretical calculations favor the formation of a six-coordinate side-on bound peroxo complex in which two acetates of edta dissociate from the metal center.[17] However, there are also other examples now available in the literature for which the formation of pentadentate seven-coordinate side-on bound peroxo complexes of Fe(III) is favored.[1]

As indicated in Figure S3, the forward reaction also occurs in the absence of general acid-catalysis. Hydrogen peroxide apparently directly attacks the $[Fe(edta)OH]^{2-}$ complex as shown in Scheme 1. It can act as a H^+ donor for protonation of the hydroxo complex to form the labile aqua complex.

(31) Chen, K.; Costas, M.; Kim, J.; Tipton, A. K.; Que, L. *J. Am. Chem. Soc.* **2002**, *124*, 3026−3035.
(32) Chen, K.; Que, L. *J. Am. Chem. Soc.* **2001**, *123*, 6327−6337.
(33) Meier, R. Habilitationsschrift, Universität Leipzig, 2002.

Theoretically, the solvent water could also function as H^+ donor, but with a pK_a of 11.6 (and even lower if coordinated to the metal center) hydrogen peroxide is a much stronger acid and overrules the acidity of water (pK_a of 15.7). At higher pH, this pathway is not available anymore since H_2O_2 is then largely deprotonated.

The suggested reaction mechanism also explains why the reaction does not occur at a low pH. The intermediate $[Fe^{III}(edta)(H_2O_2)]^-$ complex is formed via a dissociative interchange reaction of the aqua complex, in which H_2O_2 has to compete with a large excess of water to coordinate to the metal center. As the hydrogen peroxide complex is formed at lower pH, it cannot be stabilized via deprotonation due to the high H^+ concentration and decomposes immediately. This is confirmed by the observation that k_{1obs} increases steadily on decreasing the pH toward the pK_a value of the $Fe^{III}(edta)H_2O$ complex, accompanied by a decrease in the observed spectral changes, due to the acceleration of the back reaction. This also accounts for the fact that no peroxo intermediate could be observed for the reaction of $[Fe^{III}(edta)H_2O]^-$ with dioxygen and H_2O_2,[34] which was studied at pH values ≤ 6.

With the values of K_1 from eq 1 and K_B, K for the deprotonation of $[Fe(edta)H_2O]^-$ by B can be calculated as indicated in the following set of equations.

$$[Fe(edta)H_2O]^- \overset{K_1}{\rightleftharpoons} [Fe(edta)OH]^{2-} + H^+$$

$$B + H^+ \overset{K_B}{\rightleftharpoons} BH^+ \qquad K_B = 1/K_a$$

$$[Fe(edta)H_2O]^- + B \overset{K}{\rightleftharpoons} [Fe(edta)OH]^{2-} + BH^+$$

$$K = K_1K_B = K_1/K_a$$

$$pK = pK_1 - pK_a$$

Values of K were found to be $K_{TAPS} = 10$, $K_{taurine} = 45$, $K_{AMPSO} = 50$, $K_{glycine} = 250$, and $K_{CAPS} = 795$, from which it follows that the equilibrium lies more on the side of the labile aqua complex with increasing acid strength of the employed buffer, in agreement with the observations made in the kinetic study.

Similar considerations can be applied to the acid-catalyzed back reaction.

$$[Fe(edta)(H_2O_2)]^- \overset{K_C}{\rightleftharpoons} [Fe(edta)OOH]^{2-} + H^+$$

$$B + H^+ \overset{K_B}{\rightleftharpoons} BH^+ \qquad K_B = 1/K_a$$

$$[Fe(edta)(H_2O_2)]^- + B \overset{K_D}{\rightleftharpoons} [Fe(edta)OOH]^{2-} + BH^+$$

The pK_C value for coordinated H_2O_2 is unknown, but it can be estimated approximately. The back reaction is more affected by general acid-catalysis, so K_D must be smaller than K. Under the assumption of a 20% decline in K_D compared to K, the pK_C value for coordinated hydrogen peroxide can be estimated according to pK_C = pK_D + pK_a to be 7.6. This value nicely fits the expectation that coordinated hydrogen peroxide should have a significantly smaller pK_a value than free H_2O_2.

Conclusions

The results of this study clearly indicate that the reaction of Na[Fe(edta)] with hydrogen peroxide occurs in a two-step process, of which the second, $[H_2O_2]$-independent step was observed for the first time. The significant role of general acid-catalysis, which was reported before,[13] was confirmed, and in addition, a small contribution of specific acid-catalysis for the first reaction step was found. Furthermore, it was found that under certain experimental conditions the acidic form of the buffer also has a catalytic effect on the dechelation reaction of the Fe(edta)−peroxo product. Activation parameters for all reaction steps were reported. In combination with all the other kinetic data available, a detailed reaction mechanism could be presented. For the first reaction step, a dissociative interchange mechanism for both forward and back reactions can be postulated, which is controlled by the substitution behavior of the $[Fe^{III}(edta)H_2O]^-$ unit. Chelation of coordinated peroxide from end-on to side-on follows an associative interchange process accompanied by dissociation of one of the carboxylates on edta, whereas dechelation of the peroxo ligand follows a dissociative interchange process with the dissociated acetate arm of the edta ligand in the pentadentate seven-coordinate peroxo complex.

To gain further insight into the substitution behavior of iron(III) polyaminecarboxylate complexes with hydrogen peroxide, the reaction of $[Fe(cdta)H_2O]^-$ (cdta = *N*,*N*′,*N*″,*N*‴-(1,2-cyclohexanediamine)tetraacetate) with H_2O_2 will be investigated using different stopped flow techniques. Since the pK_a value of this complex (viz. 9.32)[27] is nearly two units above that of $[Fe(edta)H_2O]^-$, a significantly higher concentration of the corresponding aqua complex should be present in the pH range investigated in this study. This higher fraction of aqua complex should increase the reactivity of $[Fe(cdta)H_2O]^-$ significantly as compared to $[Fe(edta)H_2O]^-$.

Acknowledgment. The authors gratefully acknowledge financial support from the Deutsche Forschungsgemeinschaft (SFB 583 and SPP 1118) and the Max-Buchner Forschungsstiftung.

Supporting Information Available: Further mechanistic information on the reaction between Fe^{III}(edta) and hydrogen peroxide. This material is available free of charge via the Internet at http://pubs.acs.org.

IC0497580

(34) Seibig, S.; van Eldik, R. *Inorg. Chem.* **1997**, *36*, 4115−4120.